

EFFECT OF VIBRATION DATA PREPROCESSING FOR FLUTTER MARGIN PREDICTION

Masato TAMAYAMA⁺¹, Kenichi SAITOH⁺¹, Norio YOSHIMOTO⁺¹ and Hitoshi ARIZONO⁺¹
⁺¹Japan Aerospace Exploration Agency, JAXA, Tokyo, JAPAN

Although airplane's model certification must be proved by showing enough damping margin at every flight condition, the damping is not a reliable index to conduct flight tests safely, i.e. it might change drastically against the flight condition. Flight tests should stand on much more reliable index rather than damping. In this study, the Discrete Flutter Margin is used. Whichever index is used during the flight test, the accuracy of index might be influenced by the original vibration data of structures. For this purpose, two methods are taken in this study: the Random Decrement (RDD) method and the Natural Excitation Technique (NExT), each of which can effectively reduce the structural response caused by a random noise. By applying each of the RDD and the NExT processing methods to the original data, the resultant signal becomes the structural quasi-step or quasi-impulse responses. For the method to identify the system model from step and impulse responses, the Eigen-system Realization Algorithm (ERA) suits well. In this study, two sets of system identification procedures are applied to the wind tunnel experimental data: one is the combination of the RDD and the ERA, and another is the combination of the NExT and the ERA. The wind tunnel model is the half-spanned wing model of Super Sonic Transport (SST) Airplane. The test data are acquired in the JAXA's 0.6m×0.6m Transonic Flutter Wind Tunnel. The resultant Discrete Flutter Margin values acquired from both sets of procedures are compared.

Keyword: Flutter Prediction, System Identification

1. INTRODUCTION

Flight tests are definitely required in the Aeroelastic stability requirements of airworthiness regulations such as the Federal Aviation Administration Regulations, FAR. The flight tests are conducted by exploring in more severe test conditions in level flight. At every moment, therefore, the safety flight is required. Airplane's model certification must be proved by having enough damping margin in every flight condition, and damping, therefore, should be monitored to see the aeroelasticity instability. On the other hand, the damping is not a reliable index to conduct flight tests safely, i.e. it might change drastically against the flight condition. Flight tests should stand on much more reliable index rather than damping. For this purpose, the Discrete Flutter Margin, F_z , was proposed by Torii¹⁾ utilizing a system identification technique: the Auto-Regressive Moving Average (ARMA) modeling was used in his research. Whichever index is monitored in flight tests, the accuracy of index might be influenced by the original vibration data of flying airplane. The Random Decrement (RDD) method and the Natural Excitation Technique (NExT) are introduced independently to improve the prediction accuracy of aeroelasticity instability. Each of both methods can effectively reduce the structural response caused by a random noise. By applying each of the RDD and the NExT processing to the original data, the resultant signals become the structural quasi-step and quasi-impulse responses respectively. For the method to identify the system model from step and impulse responses, the Eigen-system Realization Algorithm (ERA) suits well.

In this study, two combinations of system identification procedures, {RDD and ERA} and {NExT and ERA}, were applied to the wind tunnel experimental data. The resultant F_z values were compared from a viewpoint of flutter prediction accuracy.

Most of the description, figures and tables shown in this paper is referring to the Ref.2.

⁺¹masato@chofu.jaxa.jp

2. PROCESSING METHOD

In this section, the processing methods used in this study are explained. In our study, the processes are conducted in the discrete time domain.

(1) Random Decrement Method: RDD

The RDD process proposed by Cole³⁾ is referred in this study. Suppose structural vibration data history, $\{y\}$, as shown in Fig.1 (a), which is usually measured with accelerometers or strain gauges. An offset $-y_s$ is applied to $\{y\}$, and $\{y_0\}$ is generated as follows:

$$y_0 = y - y_s \quad (1)$$

If $-y_s$ is taken appropriately, $\{y_0\}$ crossing $y_0=0$ exists at the time series $\{t_n \mid n=1 \sim N\}$. Here, both points on the time history showing plus and minus slopes are picked up. The next process is to extract a certain length data beginning from t_n as shown in Fig.1 (b). The RDD signal, $\{D\}$, is acquired by simply taking an average of these N sets of data:

$$D(m) = \frac{1}{N} \sum_{n=1}^N y_0(t_n + m - 1), \quad m = 1, 2, \dots, L \quad (2)$$

where, L is the number of data samples captured in one data set. If the structure is linear against external forces, $\{D\}$ approaches the structure's response against the external step force of $-y_s$ height. In the ERA processing, the system model must be identified based on an impulse response. To meet this requirement, $\{D\}$ is differentiated as follows:

$$\left. \begin{aligned} \hat{Y}(0) &= 0 \\ \hat{Y}(m) &= \frac{D(m+1) - D(m)}{-y_s}, \quad m = 1, 2, \dots, L-1 \end{aligned} \right\} \quad (3)$$

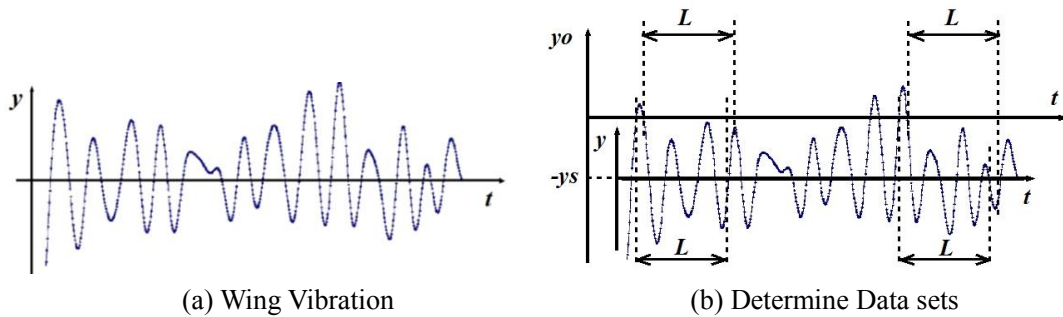


Figure 1: Time History Extraction in RDD processing

(2) Natural Excitation Technique: NExT

The mathematical background of NExT was given by James et al.⁴⁾ Consider the cross-correlation function of vibration data under a white noise excitation, $R_{ij}(t)$, between two different points of a structure, e.g. points i and j . $R_{ij}(t)$ satisfies the homogeneous equation of motion of the corresponding vibration system, and, therefore, the system characteristics can be identified from $R_{ij}(t)$. For the ERA processing, $R_{ij}(t)$ can be used directory instead of the system impulse response.

(3) Eigen-system Realization Algorithm: ERA

The Linear Time-Invariant state-space model in discrete time domain is written as follows:

$$\left. \begin{aligned} X(n+1) &= A \cdot X(n) + B \cdot u(n) \\ Y(n) &= C \cdot X(n) + D \cdot u(n) \end{aligned} \right\} \quad n = 0, 1, 2, \dots \quad (4)$$

An impulse input at zero state will cause the response known as the Markov parameter $\{Y\}$:

$$Y(n) = C \cdot A^{n-1} \cdot B \quad (5)$$

The Hankel matrix is constructed by windowing $\{Y\}$ and piling it in the row direction:

$$H_{rs}^{n-1} = \begin{bmatrix} Y(n) & \cdots & Y(n+s-1) \\ Y(1+n) & \cdots & Y(1+n+s-1) \\ \vdots & \ddots & \vdots \\ Y(r-1+n) & \cdots & Y(r-1+n+s-1) \end{bmatrix} \quad (6)$$

where 's' is the windowing length and 'r' is the number of time steps to shift the data window. In the system identification process, the Markov parameter is replaced by measured time-series data, $\{\hat{Y}\}$:

$$\hat{H}_{rs}^{n-1} = \begin{bmatrix} \hat{Y}(n) & \cdots & \hat{Y}(n+s-1) \\ \hat{Y}(1+n) & \cdots & \hat{Y}(1+n+s-1) \\ \vdots & \ddots & \vdots \\ \hat{Y}(r-1+n) & \cdots & \hat{Y}(r-1+n+s-1) \end{bmatrix} \quad (7)$$

Then, singular value decomposition is applied to \hat{H}_{rs}^0 :

$$\hat{H}_{rs}^0 = \hat{U}\hat{\Sigma}\hat{V}^T \quad (8)$$

The state-space realization is obtained by using the one step time-shifted Hankel matrix \hat{H}_{rs}^1 :

$$A = \hat{\Sigma}^{-1/2}\hat{U}^T\hat{H}_{rs}^1\hat{V}\hat{\Sigma}^{-1/2}, \quad B = \hat{\Sigma}^{1/2}\hat{V}^T E_m, \quad C = E_p^T\hat{U}\hat{\Sigma}^{1/2}, \quad D = \hat{Y}(0) \quad (9)$$

where, for the SISO system, E_m and E_p are $\{1,0,\dots,0\}^T$ sized $s \times 1$ and $\{1,0,\dots,0\}^T$ sized $r \times 1$ respectively. ' $\hat{\Sigma}$ ' is the matrix in which all of diagonal elements are non-zero and the others are zero. For the case of considering N_m structural modes, $\hat{\Sigma}$ can be truncated into the square matrix sized $2N_m \times 2N_m$. In this study, N_m was set to 3. The characteristic equation of state-space model is constructed from the eigenvalue analysis of the system state equation. The eigenvalues of discrete system, $\{\lambda_j, \lambda_j^* \mid j=1 \sim N_m\}$, where '*' indicates complex conjugate transpose, are also used to calculate modal frequencies, $\{f_j \mid j=1 \sim N_m\}$, and damping ratios, $\{\zeta_j \mid j=1 \sim N_m\}$:

$$f_j = \frac{|\lambda_{Cj}|}{2\pi}, \quad \zeta_j = -\frac{\text{real}(\lambda_{Cj})}{|\lambda_{Cj}|} \quad j=1,2,\dots,N_m \quad : \quad \lambda_{Cj} = \frac{\ln(\lambda_j)}{\Delta t} \quad (10)$$

where Δt is the sampling time interval.

(4) Discrete Flutter Margin

The discrete flutter margin was proposed by Torii.¹⁾ Consider the system characteristic equation in discrete time domain:

$$G(z) = A_6 z^6 + A_5 z^5 + A_4 z^4 + A_3 z^3 + A_2 z^2 + A_1 z + A_0 \quad (11)$$

where the order of equation is 6, and the equation have 3 conjugate pairs of poles. For this system, the Jury's stability criteria is expressed as follows:

$$\left. \begin{aligned} G(1) &= A_6 + A_5 + A_4 + A_3 + A_2 + A_1 + A_0 > 0 \\ G(-1) &= A_6 - A_5 + A_4 - A_3 + A_2 - A_1 + A_0 > 0 \end{aligned} \right\} \quad (12)$$

and also,

$$\left. \begin{aligned} F_1^+ &\equiv A_6 + A_0 > 0, \quad F_1^- \equiv A_6 - A_0 > 0 \\ F_5^+ &\equiv \det(S+T) > 0, \quad F_5^- \equiv \det(S-T) > 0 \end{aligned} \right\} \quad (13)$$

$$S = \begin{bmatrix} A_6 & A_5 & A_4 & A_3 & A_2 \\ 0 & A_6 & A_5 & A_4 & A_3 \\ 0 & 0 & A_6 & A_5 & A_4 \\ 0 & 0 & 0 & A_6 & A_5 \\ 0 & 0 & 0 & 0 & A_6 \end{bmatrix}, \quad T = \begin{bmatrix} A_4 & A_3 & A_2 & A_1 & A_0 \\ A_3 & A_2 & A_1 & A_0 & 0 \\ A_2 & A_1 & A_0 & 0 & 0 \\ A_1 & A_0 & 0 & 0 & 0 \\ A_0 & 0 & 0 & 0 & 0 \end{bmatrix} \quad (14)$$

Then the Discrete Flutter Margin, F_z , is constructed with the parameters acquired in Eq. (13):

$$F_z \equiv \frac{F_5^-}{(F_1^-)^2} = \frac{d e (S - T)}{(A_6 - A_0)^2} \tag{15}$$

3. RESULTS AND DISCUSSIONS

The experimental model is the low aspect ratio semi-spanned wing with an engine nacelle. Figure 2 shows the planform of model. The airfoil shape is NACA0006 at every span section. Four strain gauges, #1 through #4, are attached at the locations shown in Fig.2. The wing’s first three structural eigen-modes are shown in Tab.1 accompanied with their natural frequencies. The tests were conducted at the Transonic Flutter Wind Tunnel in JAXA, whose specification is shown in Tab.2. The bottom graph in Fig.3 shows the time history of strain gauge. The test was conducted at the nominal Mach number of 0.90: the time history of free stream Mach number is also shown in Fig.3. The dynamic pressure, q , was changed by sweeping the total pressure, P_0 , with the speed of 6 kPa/s from 200 kPa to 300 kPa, and then 3 kPa/s from 300 kPa. Strain data were sampled at a frequency of 5 kHz after 1 kHz low pass filtering. The flutter occurred at $q = 109$ kPa with a mild vibration. Figure 4 shows the spectrogram of strain gauge signal. The 1st structural mode increases its frequency as q increases.

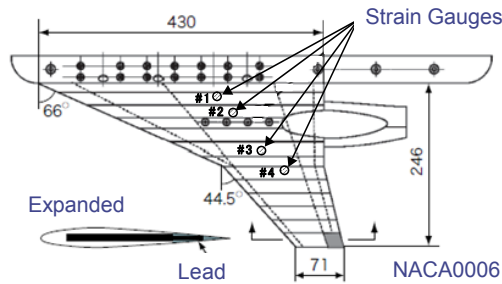


Figure 2: Plan View of Wing Model

Table 1: Eigen-modes and frequencies (Vibration Tests)

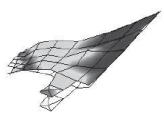
1st Mode	2nd Mode	3rd Mode
77[Hz]	126[Hz]	196[Hz]
		

Table 2: Specification of Wind Tunnel

Type	Blow Down
Operation Range	M : 0.5 ~ 1.2 Po : 150 ~ 400 kPa Re : ~ 6.0x10 ⁷ /m Dynamic Pressure : 22 ~ 166 kPa
Test Section	0.6m x 0.6m
Test Period	~ about 120 s
Mass Flow Rate	~ 320kg/s

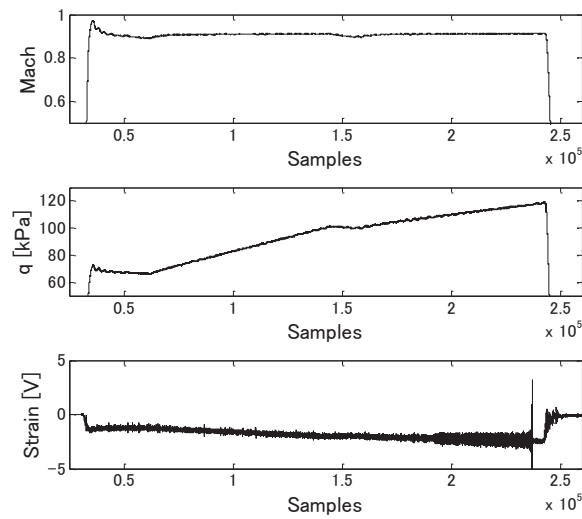


Figure 3: Results of Wind Tunnel Tests

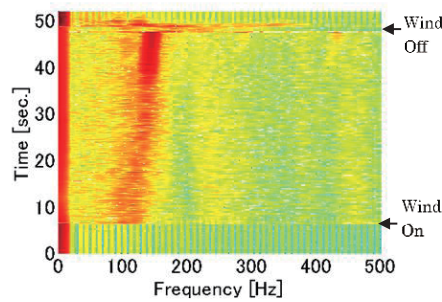


Figure 4: Spectrogram of Strain Gauge Signal

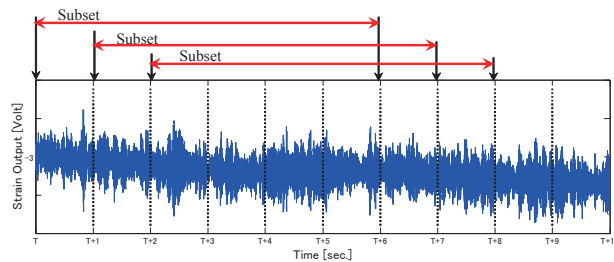


Figure 5: Data 'Subset' in the RDD Processing

(1) Application of RDD and NExT

The RDD and NExT were applied to the vibration signals of 6 sec. period, which is named here as 'subset.' As shown in Fig.5, each subset starts 1 sec. delayed from the former subset. The threshold level, y_s , was set to $1.4\sigma_m$: σ_m is the standard deviation of the corresponding subset signal. In order to include only 3 structural modes in the vibration signal, the measured signal was applied with digital band-pass filtering designed with Butterworth filter; from 100 Hz through 260 Hz for the RDD, and from 100 Hz through 280 Hz for the NExT. Although there is a discrepancy of the upper pass frequencies between each method, these values gave the best result in this study. Figure 6 (b) shows the example processed with the subset indicated in Fig.6 (a). Both results of the RDD and the NExT show almost the same decaying time histories. Figure 6 (c) is the power spectrums of both processed results. The RDD processing shows high values for higher structural

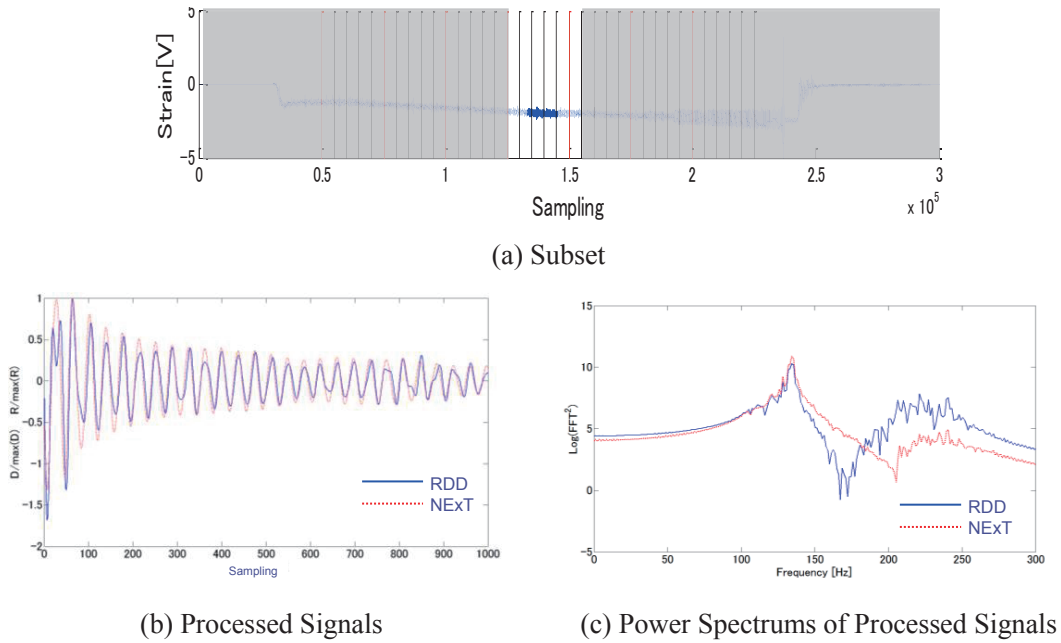


Figure 6: Example of RDD and NExT Processing

modes comparing to the NExT processing.

(2) System Identification by ERA

The size of Hankel matrix was set to 10×150 referring to Tamayama et al.⁵⁾ Figure 7 shows the Modal Amplitude Coherence (MAC) to see the accuracy of system identification by the ERA. The MAC for the *i* th mode is defined as the coherence between the measured modal amplitude history and the identified one.⁶⁾ The former one for the *i* th mode, \bar{q}_i , is calculated directly from the decomposition of Hankel matrix. The latter one, \hat{q}_i , is calculated from the initial modal amplitudes, which is also presented by the decomposition of Hankel matrix, and the eigenvalues of identified state matrix. The MAC is defined by the following equation:

$$MAC_i = \frac{|\bar{q}_i^* \cdot \hat{q}_i|}{\left((\bar{q}_i^* \cdot \bar{q}_i) \cdot (\hat{q}_i^* \cdot \hat{q}_i) \right)^{1/2}} \tag{16}$$

where ' * ' indicates complex conjugate transpose. The MAC takes a value between 0 and 1. The more accurate the system identification was performed, the more the MAC value becomes close to 1. From Fig.7, the MAC for both methods of RDD and NExT gives over 0.96. The hatched area is supercritical condition and out of consideration in this research. The ERA identification is considered to have been properly conducted for both of RDD and NExT processed signals.

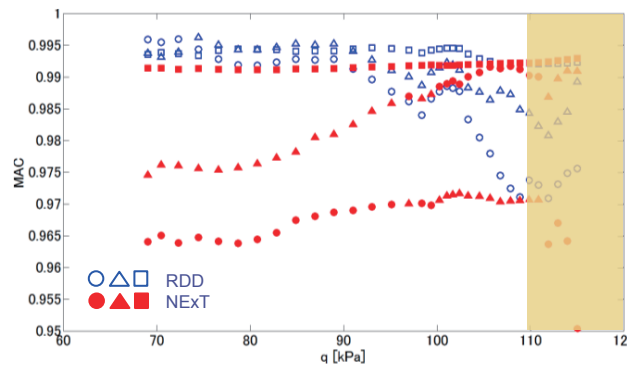


Figure 7: Modal Amplitude Coherence (MAC) ○●:1st Mode, ▲△:2nd Mode, □■:3rd Mode

Figures 8(a) and (b) show the change of modal characteristics as q increases. The modal frequencies of 1st and 3rd modes show good agreement between the RDD and the NExT results. The 2nd mode frequency shows larger decrease for the NExT result than the RDD one. The modal damping ratio of 1st mode decreases suddenly beyond $q = 100$ kPa for both of the RDD and the NExT results.

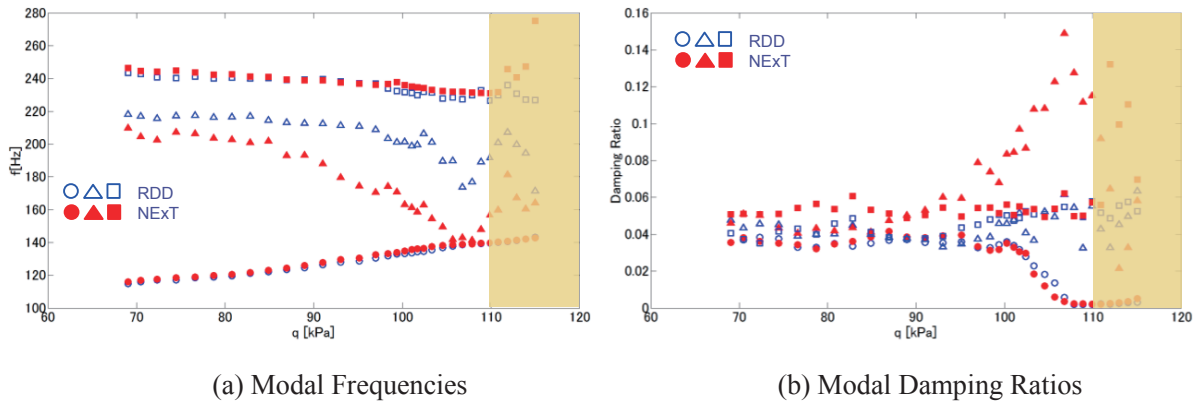


Figure 8: Modal Characteristics ○●:1st Mode, ▲▲:2nd Mode, □■:3rd Mode

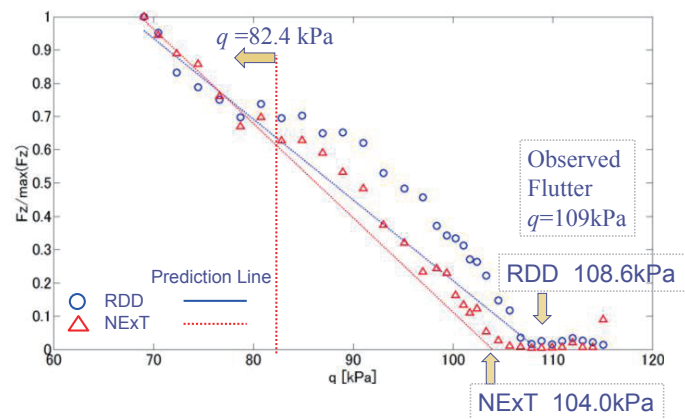


Figure 9: Flutter Condition Prediction

(3) Discrete Flutter Margin and Flutter Condition Prediction

Figure 9 shows F_z distribution against q . The lines in the figure show the linear fittings drawn from F_z calculated below $q = 82.4$ kPa, which is correspond with the 15% velocity margin from the experimentally observed flutter speed. In order to compare the values calculated from different methods, the vertical axis is normalized by the maximum values for each method. Prediction with the RDD shows closer prediction to the actual flutter dynamic pressure than that with the NExT. The standard deviations around the prediction line were calculated for each of the RDD and the NExT; 0.0717 for the RDD and 0.0428 for the NExT. The linearity of F_z is well for the NExT than the RDD.

4. CONCLUDINGS

The demonstration of flutter prediction from the Discrete Flutter Margin was presented in this study. The prediction was conducted by identifying the system model by the ERA. This identification method needs an impulse response of the corresponding structure. For this requirement, two different methods were compared in this study. One is the RDD, and another is the NExT. Followings are presented as the conclusions:

- (1) The RDD seems to have stronger signal at higher frequencies comparing to the NExT,

- (2) The ERA seems to have identified the system model appropriately for each of the RDD and the NExT considering from the Modal Amplitude Coherence, MAC,
- (3) Prediction with the NExT shows more linear relationship against the dynamic pressure than the RDD.

REFERENCES

- 1) Torii, H. : Application of Discrete-Time Flutter Prediction Method to a Three-Mode System, *the International Forum on Aeroelasticity and Structural Dynamics 2011*.
- 2) Tamayama, M. : Comparison between Random Decrement Method and Natural Excitation Technique as a Preprocessor of Flutter Margin Prediction Program, *the International Conference in Nonlinear Problems in Aviation and Aerospace 2014*.
- 3) Cole, H. A., Jr. : On-line Failure Detection and Damping Measurement of Aerospace Structures by Random Decrement Signatures, *NASA CR-2205*, 1973.
- 4) James, G. H., Carrie, T. G. and Lauffer, J. P. : The Natural Excitation Technique (NExT) for Modal Parameter Extraction From Operating Wind Turbines, *SANDIA REPORT*, SAND92-1666, 1993.
- 5) Tamayama, M., Arizono, H., Saitoh, K. and Yoshimoto, N. : Flutter Margin Prediction by Combination of Random Decrement Method and Eigen-system Realization Algorithm, *the International Forum on Aeroelasticity and Structural Dynamics 2013*.
- 6) Juang, J. N. and Pappa, R. S. : An Eigensystem Realization Algorithm for Modal Parameter Identification and Modal Reduction, *Journal of Guidance, Control, and Dynamics*, Vol.8, No.5, p.p.620-627, 1985.